



## Short communication

# Sulfonated reduced graphene oxide as a highly efficient catalyst for direct amidation of carboxylic acids with amines using ultrasonic irradiation



Maryam Mirza-Aghayan<sup>a,\*</sup>, Mahdieh Molaee Tavana<sup>a</sup>, Rabah Boukherroub<sup>b</sup>

<sup>a</sup> Chemistry and Chemical Engineering Research Center of Iran (CCERC), P.O. BOX 14335-186, Tehran, Iran

<sup>b</sup> Institut d'Electronique, de Microélectronique et de Nanotechnologie (IEMN, UMR 8520), Avenue Poincaré – CS 60069, 59652 Villeneuve d'Ascq, France

## ARTICLE INFO

## Article history:

Received 6 August 2015

Received in revised form 12 October 2015

Accepted 12 October 2015

Available online 22 October 2015

## Keywords:

Sulfonated reduced graphene oxide

Carboxylic acids

Amines

Direct amidation

Solid acid catalyst

Sonochemical reaction

## ABSTRACT

Sulfonated reduced graphene oxide nanosheets (rGO-SO<sub>3</sub>H) were prepared by grafting sulfonic acid-containing aryl radicals onto chemically reduced graphene oxide (rGO) under sonochemical conditions. rGO-SO<sub>3</sub>H catalyst was characterized by Fourier-transform infrared (FT-IR) spectroscopy, Raman spectroscopy, scanning electron microscopy (SEM), X-ray diffraction (XRD), thermogravimetric analysis (TGA), differential scanning calorimetry (DSC) and X-ray photoelectron spectroscopy (XPS). rGO-SO<sub>3</sub>H catalyst was successfully applied as a reusable solid acid catalyst for the direct amidation of carboxylic acids with amines into the corresponding amides under ultrasonic irradiation. The direct sonochemical amidation of carboxylic acid takes place under mild conditions affording in good to high yields (56–95%) the corresponding amides in short reaction times.

© 2015 Elsevier B.V. All rights reserved.

## 1. Introduction

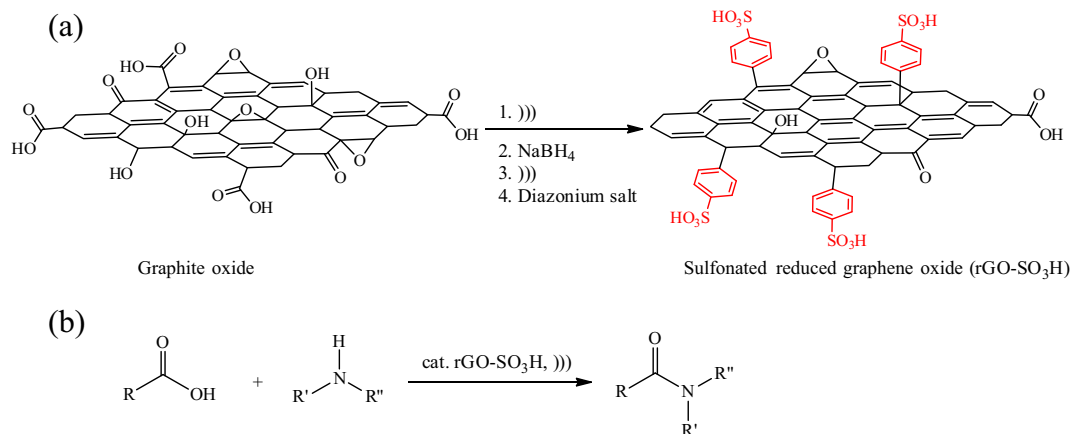
Amide is one of the most important functional groups in organic chemistry; amides are present in many natural products, peptides, synthetic polymers, pharmaceuticals, and biological systems [1]. Several amide derivatives have biological properties such as anti-tumor, antifungal, antihistamine, anthelmintic, and antibacterial activity [2,3]. They are also useful and valuable intermediates for the synthesis of various important compounds [4]. Usually amides can be synthesized by the reaction of carboxylic acids [5] or their derivatives such as halides [6], esters [7], and carboxylic salts [8] with amines. A number of methods have been developed for the synthesis of amide compounds, including rearrangement of aldoximes [9], transamidation of amides with amines [10,11], cross coupling of amides with aryl halides [12], aminocarbonylation of aryl halides [13] or terminal alkynes [14], hydration of nitriles [15] and Ugi reaction [16]. The catalytic procedures developed for oxidative amidation of aldehydes [17], alcohols [18–21] and alkylarenes [22] with amines or amine salts are quite attractive from atom economy and green chemistry view points. Recently, *N*-heterocyclic carbene (NHC)-catalyzed oxidative amidation of aromatic aldehydes with amines in the presence of *N*-bromosuccinimide as an

oxidant has been proposed for the synthesis of amides [17]. Bantreil et al. established a domino reaction for the formation of benzamides in one step from various benzyl alcohols in the presence of copper salt [18]. Recently, Wang et al. investigated direct oxidative amidation between methylarenes and free amines in water by employing *tert*-butyl hydroperoxide as the environmental benign oxidant with the co-catalysis of tetrabutyl-ammonium iodide and FeCl<sub>3</sub> in the presence of 4 Å molecular sieves [22]. Nevertheless, some of the reported methods require stoichiometric amounts of coupling reagents and suffer from poor atom efficiency or the use of highly hazardous reagents. Despite the low reactivity of acids, direct amidation is still the most preferred industrial process from both atom economy and environmental points of view. Thus, it is desirable to use a cheap and environmentally benign catalyst for direct amidation in order to overcome these problems.

Solid acids have the great potential to replace liquid acids as environmentally benign acid catalysts [23,24]. Acidic carbons, based on the concept of green chemistry, were investigated as stable and highly active protonic acid catalysts for several acid-catalyzed reactions [25,26]. Graphene oxide and graphite oxide have been effectively applied as useful heterogeneous catalysts for certain organic transformations [27–32]. Recently, we have demonstrated the efficiency of graphite oxide as a solid acid catalyst for esterification of organic acids with alcohols [33] and ring-opening of epoxides with various alcohols [34].

\* Corresponding author.

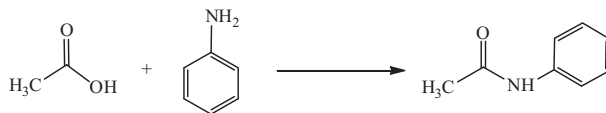
E-mail address: [m.mirzaaghayan@ccerci.ac.ir](mailto:m.mirzaaghayan@ccerci.ac.ir) (M. Mirza-Aghayan).



**Scheme 1.** (a) Synthesis of rGO-SO<sub>3</sub>H; (b) direct sonochemical amidation of carboxylic acids with amine derivatives using rGO-SO<sub>3</sub>H catalyst.

**Table 1**

Different conditions for the direct amidation of acetic acid with aniline<sup>a</sup>.



Entry	Catalyst	Conditions	Time	Yield (%)
1	–	Solvent-free, room temperature	72 h	20
2	–	Acetonitrile, reflux	48 h	32
3	Graphite oxide (5 mg)	Solvent-free, room temperature	48 h	29
4	rGO-SO <sub>3</sub> H (5 mg)	Solvent-free, room temperature	8 h	45
5	rGO-SO <sub>3</sub> H (5 mg)	Solvent-free, 70 °C	2 h	86
6	rGO-SO <sub>3</sub> H (5 mg)	Bath ultrasonic, solvent-free, 70 °C	20 min	92
7	rGO-SO <sub>3</sub> H (5 mg)	Bath ultrasonic, solvent-free, room temperature	20 min	94
8	–	Bath ultrasonic, solvent-free, room temperature	100 min	–
9	Graphite oxide (5 mg)	Bath ultrasonic, solvent-free, room temperature	20 min	8
10	rGO-SO <sub>3</sub> H (2.5 mg)	Bath ultrasonic, solvent-free, room temperature	20 min	27

<sup>a</sup> Reaction conditions: acetic acid (1 mmol) and aniline (1 mmol).

Sonochemical waves were employed to exfoliate graphite oxide and functionalized graphene oxide. An original approach was recently proposed by Maktedar et al. for the direct functionalization of graphene oxide with 6-aminoindazole through sonochemical nucleophilic substitution reaction [35]. Wang et al. applied sulfonated graphene as a solid catalyst for the ester-exchange reaction [36]. Sulfonated graphene catalyst prepared by grafting sulfonic acid-containing aryl radicals onto the two-dimensional surface of graphene was successfully used for the etherification of glycerol with isobutene [37].

In continuation of our efforts on the use of graphite oxide, we investigate in this work a simple procedure for the preparation of sulfonated reduced graphene oxide (rGO-SO<sub>3</sub>H) (Scheme 1a). The catalytic activity of rGO-SO<sub>3</sub>H as a reusable solid acid catalyst was further investigated for the direct amidation of carboxylic acids with amines into the corresponding amides under ultrasonic irradiation (Scheme 1b). Although the effect of ultrasound in chemical reactions is known [38], to the best of our knowledge, there are only a few examples on the amidation reaction [39–41].

## 2. Experimental section

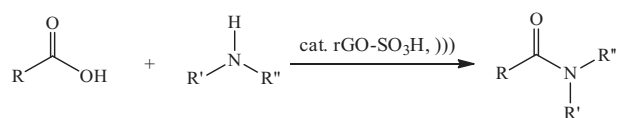
### 2.1. Analysis and characterization of materials used in this study

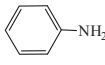
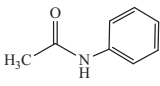
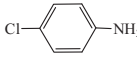
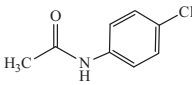
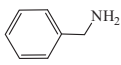
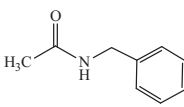
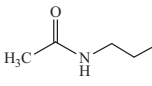
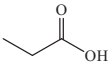
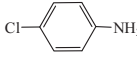
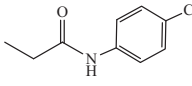
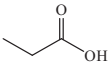
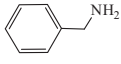
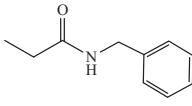
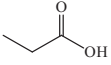
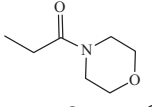
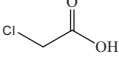
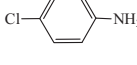
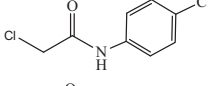
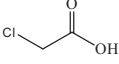
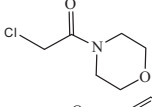
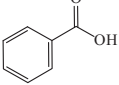
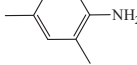
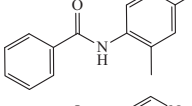
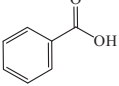
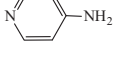
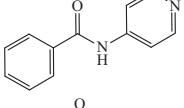
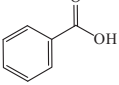
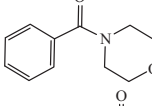
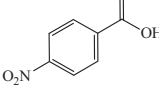
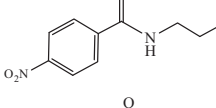
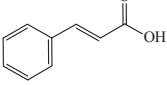
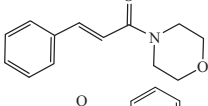
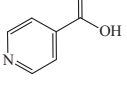
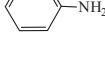
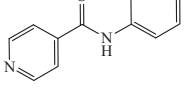
Ultrasonic irradiation was accomplished with an Elmasonic P ultrasonic cleaning unit (bath ultrasonic) with a frequency of 37 kHz and 100% output power. IR spectra were recorded from

KBr disks with a Bruker Vector 22 FT-IR spectrometer. Raman spectra were recorded using a dispersive Raman spectrophotometer Bruker model SENTERRA. Scanning electron microscopy (SEM) and energy dispersive X-ray (EDX) data were obtained using a VEGA3 LMU TESCAN SEM. X-ray diffraction (XRD) data were performed using a Bruker D8 Advance Theta-2theta diffractometer. Thermogravimetric analysis (TGA) was performed on a NETZSCH TG 209 F1. Differential scanning calorimetry (DSC) was carried out on a NETZSCH DSC 204 F1 Phoenix. X-ray photoelectron spectroscopy (XPS) were collected on a VG ESCALAB MK-II spectrometer with Al K $\alpha$  as the excitation source ( $h\nu = 1486.6$  eV) operated at 10.5 kV and 20 mA at a pressure better than  $10^{-8}$  Pa. GC–MS analysis was performed on a FISON GC 8000 series TRIO 1000 gas chromatograph equipped with a capillary column CP Sil.5 CB, 60 m  $\times$  0.25 mm i.d. <sup>1</sup>H and <sup>13</sup>C NMR spectra were recorded on a Bruker 300 and 75 MHz spectrometer using tetramethylsilane as internal standard. Elemental analyses were performed on a ThermoFinnigan Flash EA 1112 series elemental analyzer.

### 2.2. Synthesis of sulfonated reduced graphene oxide nanosheets (rGO-SO<sub>3</sub>H)

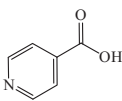
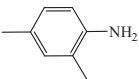
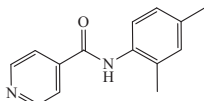
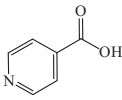
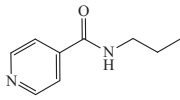
Typically, 150 mg of graphite oxide [30] powder in 150 mL water were mixed in a reaction container using bath ultrasonic with a frequency of 37 kHz for 30 min. A solution of 1.2 g NaBH<sub>4</sub> in 30 mL water was added dropwise into the graphite oxide

**Table 2**Ultrasound-assisted direct amidation of various acids with amines using rGO-SO<sub>3</sub>H catalyst.

Entry	Acid	Amine	Amide	Time	Yield <sup>a</sup> (%)
1				20	94 [9]
2				30	82 [9]
3				20	87 [47]
4				20	95 [48]
5				20	76 [12]
6				20	80 [7]
7				20	73 [7]
8				20	81 [49]
9				20	75 [50]
10				20	92 [51]
11				20	85 [52]
12				20	80 [53]
13				20	94 [54]
14				40	56 [55]
15				40	73 [55]

(continued on next page)

Table 2 (continued)

Entry	Acid	Amine	Amide	Time	Yield <sup>a</sup> (%)
16				40	81
17				40	84

<sup>a</sup> Isolated product.

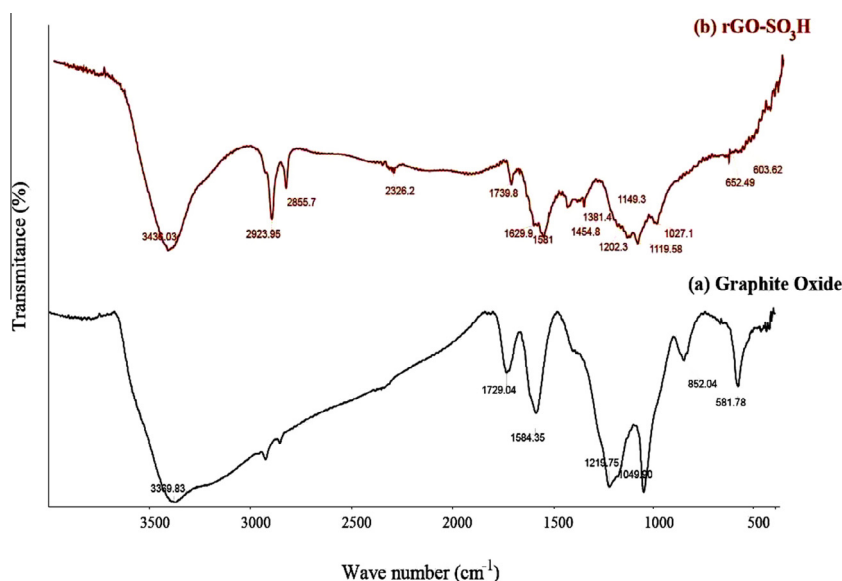


Fig. 1. FT-IR spectra of (a) graphite oxide and (b) rGO-SO<sub>3</sub>H nanosheets.

dispersion, with the pH adjusted to 9–10 by addition of 5 wt.% Na<sub>2</sub>CO<sub>3</sub> solution. The mixture was heated at 80 °C for 1 h after which the brown graphene oxide solution turned black. Next, the mixture was washed with water and centrifuged three times at 3700 rpm for 20 min. The partially reduced graphene oxide (rGO) was sonicated in 150 mL water using bath ultrasonic with a frequency of 37 kHz for 30 min and cooled in an ice bath. Then, a diazonium salt was prepared from the reaction of 92 mg sulfanilic acid and 1 mL of 1 N HCl in 10 mL water in an ice bath at 0 °C, followed by the addition of 36 mg NaNO<sub>2</sub> in 10 mL water until all reactants had dissolved. The diazonium solution was poured into the rGO solution at 0 °C and stirred overnight at room temperature. The black solution was centrifuged at 3700 rpm for 20 min and washed with deionized water three times. The resultant black residue was filtered followed by dehydration on a rotary evaporator under vacuum and dried in oven at 80 °C for 2 h.

### 2.3. Typical procedure for the direct amidation of carboxylic acids with amines under ultrasonication

To a mixture of carboxylic acid (1 mmol) and amine (1 mmol) was added rGO-SO<sub>3</sub>H (5 mg). The resulting mixture was sonicated in an Elmasonic P ultrasonic cleaning unit (ultrasonic bath) with a frequency of 37 kHz and 100% output power at room temperature for the time indicated in Table 2. Then ethyl acetate was added and the mixture was filtered through a sintered funnel and extracted with ethyl acetate. The organic layer was dried over Na<sub>2</sub>SO<sub>4</sub>, filtered and evaporated under reduced pressure. Purification was

achieved by column chromatography using *n*-hexane/EtOAc: 100/3 as eluent. The spectroscopic data of the obtained esters were compared with authentic samples. Spectroscopic data:

*N*-(2,4-dimethylphenyl)isonicotinamide (entry 16, Table 2): Colorless oil, IR (KBr)  $\nu$  = 3298, 3082, 2931, 1655, 1549, 903, 755, 693 cm<sup>-1</sup>; <sup>1</sup>H NMR (300 MHz, CDCl<sub>3</sub>)  $\delta$  = 2.69 (s, 3H, CH<sub>3</sub>), 3.36 (s, 3H, CH<sub>3</sub>), 6.79–7.02 (m, 3H, CH Arom), 7.31–7.47 (m, 4H, CH Arom), 10.30 (s, 1H, NH); <sup>13</sup>C NMR (75 MHz, CDCl<sub>3</sub>)  $\delta$  = 18.9, 24.8, 112.3, 121.9, 130.4, 132.2, 135.2, 142.1, 144.4, 152.7, 166.2; MS (EI) (70 eV),  $m/z$  (%): 226 (7) [M]<sup>+</sup>, 148 (32), 121 (100), 107 (53), 105 (5), 78 (5).

*N*-propylisonicotinamide (entry 17, Table 2): Yellow oil; IR (KBr)  $\nu$  = 3261, 3057, 2931, 1665, 1500, 961, 752, 665 cm<sup>-1</sup>; <sup>1</sup>H NMR (300 MHz, CDCl<sub>3</sub>)  $\delta$  = 0.85 (t,  $J$  = 6.6 Hz, 3H, CH<sub>3</sub>), 1.23–1.66 (m, 2H, CH<sub>2</sub>CH<sub>3</sub>), 2.91 (t,  $J$  = 7.4 Hz, 2H, CH<sub>2</sub>CH<sub>2</sub>CH<sub>3</sub>), 7.31–8.32 (m, 5H, CH Arom and NH); <sup>13</sup>C NMR (75 MHz, CDCl<sub>3</sub>)  $\delta$  = 13.2, 23.7, 42.6, 123.9, 144.8, 149.1, 166.7; MS (EI) (70 eV),  $m/z$  (%): 164 (5) [M]<sup>+</sup>, 121 (34), 106 (53), 86 (25), 78 (5), 43 (100).

## 3. Results and discussion

### 3.1. Characterization of rGO-SO<sub>3</sub>H nanosheets catalyst

The overall process of sulfonation was monitored by FT-IR spectroscopy. FT-IR spectrum of graphite oxide shows peaks at about 3369, 1729, 1584, 1219 and 1049 cm<sup>-1</sup> assigned to O–H, C=O, C=C, (C–O) epoxy and (C–O) alkoxy groups, respectively (Fig. 1) [42,43]. The comparison of FT-IR spectra of graphite oxide and

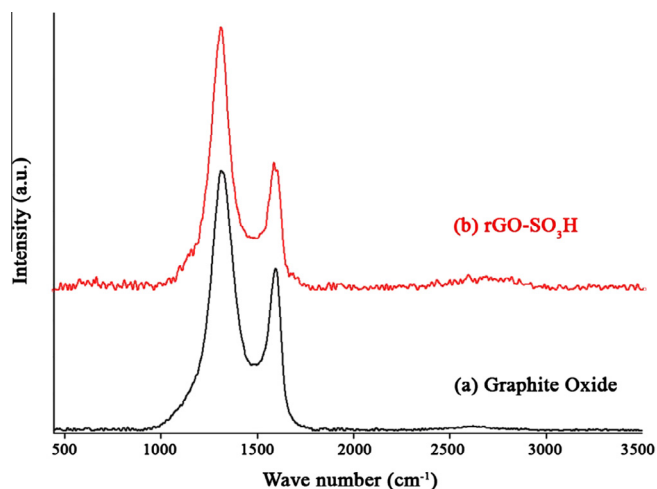


Fig. 2. Raman spectra of (a) graphite oxide and (b) rGO-SO<sub>3</sub>H nanosheets.

rGO-SO<sub>3</sub>H nanosheets evidently suggests that chemical changes occurred during its preparation. Indeed, in the rGO-SO<sub>3</sub>H FT-IR spectrum, the peak at 1729 cm<sup>-1</sup> is highly decreased, which indicates a partial reduction of graphite oxide in the sulfonation process [44]. The presence of a broad band at about 1629 cm<sup>-1</sup> due to C=C stretching modes clearly suggests partial restoration of the aromatic network during the chemical process [42,43]. The appearance of peaks at about 1381 and 1202 cm<sup>-1</sup> due to the S=O symmetric and asymmetric stretching modes, respectively confirms the successful decoration of sulfonic groups on the rGO-SO<sub>3</sub>H surface. The peaks at about 652 and 603 cm<sup>-1</sup> are associated with S—O and S—C stretching modes, respectively, signifying the existence of covalent sulfonic acid groups on the surface of rGO-SO<sub>3</sub>H nanosheets (Fig. 1) [44].

Fig. 2 shows the Raman spectra of graphite oxide and rGO-SO<sub>3</sub>H nanosheets. Two characteristic peaks at 1311 and 1594 cm<sup>-1</sup> for graphite oxide and at 1313 and 1585 cm<sup>-1</sup> for rGO-SO<sub>3</sub>H occur in each spectrum, corresponding to the D and G bands, respectively. The I<sub>D</sub>/I<sub>G</sub> ratio in rGO-SO<sub>3</sub>H (2.07) is greater than that of graphite oxide (1.56). The result suggests that some of the oxygenated groups are removed by NaBH<sub>4</sub> under sonochemical conditions.

The comparison of SEM images of graphite oxide and rGO-SO<sub>3</sub>H nanosheets confirms its exfoliation after grafting of sulfonic acid-containing aryl radicals onto chemically rGO under ultrasonication. It should be noted that the presence of sulfur with 6.25 at.% in EDX spectra suggests the presence of the sulfonated group in rGO-SO<sub>3</sub>H nanosheets (Fig. 3). CHNS analysis indicates the presence of sulfur in 4.74% in rGO-SO<sub>3</sub>H nanosheets.

The XRD pattern of graphite oxide displays a single diffraction peak at 2θ = 11.8°, suggesting the formation of graphite oxide upon graphite oxidation by the Hummer's method (Fig. 4a) [43]. After chemical reduction of exfoliated graphite oxide with NaBH<sub>4</sub> and after grafting sulfonic acid containing aryl radicals, the peak of graphite oxide at 2θ = 11.8° decreased and a new broad peak at 2θ = 26.3° appeared, confirming the formation of rGO-SO<sub>3</sub>H (Fig. 4b) [45]. This result suggests graphite oxide reduction to rGO-SO<sub>3</sub>H by partial removal of oxygenated functional groups. The interlayer spacing (d-spacing) value for graphite oxide was 0.21 nm, while the interlayer spacing of rGO-SO<sub>3</sub>H was calculated to be 0.78 nm, which revealed the increase of distance between rGO-SO<sub>3</sub>H nanosheets.

Fig. 5 displays the TGA curves of graphite oxide and rGO-SO<sub>3</sub>H samples. The overall weight loss of 51% for graphite oxide occurs in three successive steps. The first one is a steady weight loss of 7% attributed to the vaporization of adsorbed water molecules and occurs at around 100 °C. Then a rapid loss of 25% due to the decomposition of the oxygen-containing functional groups such as hydroxyl, epoxy, carbonyl, and carboxyl groups in the temperature range of 100–208 °C. Finally, a weight loss of 19% that can be

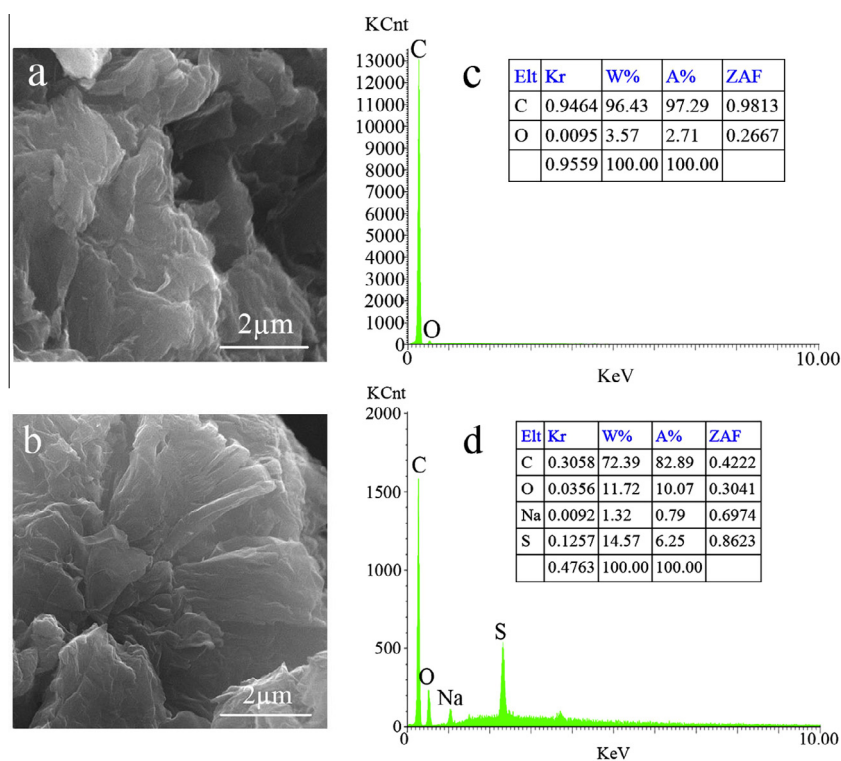


Fig. 3. SEM images (a) graphite oxide and (b) rGO-SO<sub>3</sub>H; (c) and (d) their respective EDX spectra.

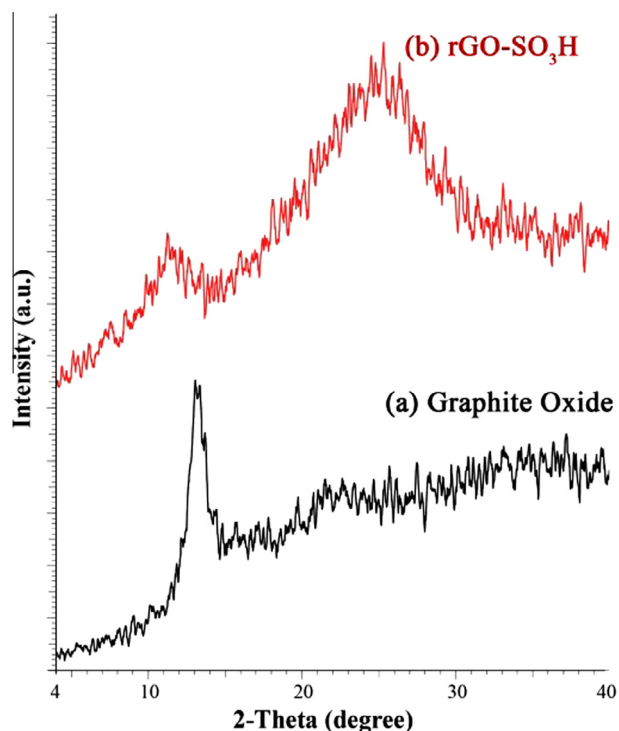


Fig. 4. XRD patterns of (a) graphite oxide and (b) rGO-SO<sub>3</sub>H nanosheets.

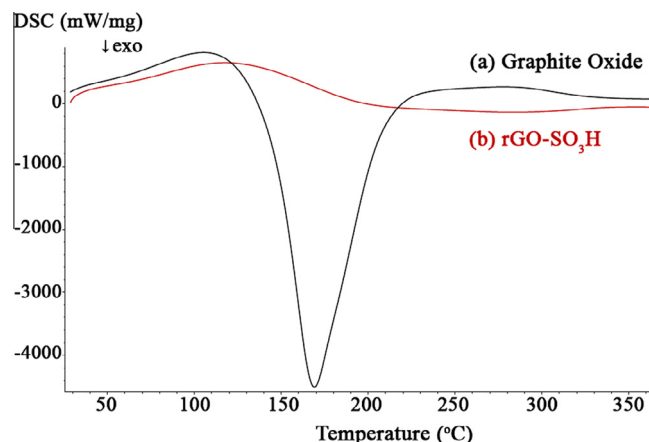


Fig. 6. DSC curves of (a) graphite oxide and (b) rGO-SO<sub>3</sub>H nanosheets.

The XPS wide-scan spectrum of rGO-SO<sub>3</sub>H nanosheets showed two peaks at 531.0 and 282.8 eV which correspond to O<sub>1s</sub> and C<sub>1s</sub>, respectively (Fig. 7a). The presence of sulfur in rGO-SO<sub>3</sub>H nanosheets was confirmed by two characteristic peaks of S<sub>2s</sub> and S<sub>2p</sub> at 214.0 and 166.1 eV, respectively [46]. High resolution XPS spectrum of S<sub>2p</sub> displays a single peak at 168.4 eV which correspond to S–O bond (Fig. 7b). This result indicated the successful incorporation of sulfur group in rGO-SO<sub>3</sub>H nanosheets. Moreover, the high resolution XPS spectrum of C<sub>1s</sub> exhibits two peaks at 284.6 and 288.8 eV corresponding to sp<sup>2</sup> C=C bonding and the carboxylic acid group, respectively (Fig. 7c). It should be noted that the characteristic peak at 286.9 eV which corresponding to C–OH and C–O–C moieties not clearly observed. This result suggests that some of the oxygenated groups in rGO-SO<sub>3</sub>H nanosheets are reduced by NaBH<sub>4</sub> under sonochemical conditions.

### 3.2. Catalytic performance of rGO-SO<sub>3</sub>H nanosheets

Initially, we screened the direct amidation of acetic acid (1 mmol) with aniline (1 mmol) under different conditions. The results are summarized in Table 1. First, the direct amidation of acetic acid (1 mmol) with aniline in absence of catalyst at room temperature in solvent-free condition or in reflux of acetonitrile afforded the corresponding amide in 20% and 32% yield after 72 and 48 h, respectively (entries 1 and 2, Table 1). When the amidation of acetic acid was performed in presence of 5 mg of graphite oxide in absence of solvent, the corresponding amide was obtained in 29% yield after 48 h (entry 3, Table 1). The amidation of acetic acid in the presence of 5 mg of rGO-SO<sub>3</sub>H at room temperature gave *N*-phenylacetamide in 45% yield after 8 h (entry 4, Table 1). Next, this reaction was carried out at 70 °C and the obtained *N*-phenylacetamide was isolated in 86% yield after 2 h (entry 5, Table 1). The comparison of entries 2 and 5 clearly indicates that rGO-SO<sub>3</sub>H catalyst has an important role in the direct amidation by decreasing the reaction time and increasing the yield. In the next step, we examined the effect of ultrasonic irradiation on this chemical transformation. The reaction was carried out in the presence of 5 mg of rGO-SO<sub>3</sub>H in an Elmasonic P ultrasonic cleaning unit (ultrasonic bath) with a frequency of 37 kHz and 100% output power at 70 °C. A decrease in the reaction time was observed; *N*-phenylacetamide was isolated in 92% yield only after 20 min (entry 6, Table 2). It should be noted that a similar result was obtained when the reaction was performed at room temperature, suggesting that room temperature was enough for this reaction (entry 7, Table 1). In the absence of rGO-SO<sub>3</sub>H, the direct amidation of acetic acid with aniline gave the starting material after 100 min

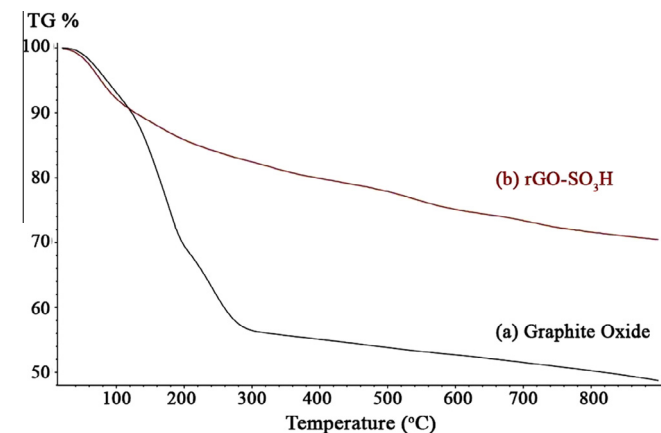


Fig. 5. TGA analysis of (a) graphite oxide and (b) rGO-SO<sub>3</sub>H nanosheets.

attributed to the combustion of the carbon skeleton is observed in the temperature range of 208–900 °C (Fig. 5a) [42]. rGO-SO<sub>3</sub>H nanosheets show overall less than 30% weight loss in the same temperature range (Fig. 5b). The weight loss of rGO-SO<sub>3</sub>H nanosheets takes place in four successive steps. The first one is a weight loss of 17% at around 300 °C and three successive steps with a slow decrease of weight loss of 12% in the temperature range of 300–900 °C. The weight loss in the temperature range 400–580 °C can be attributed to decomposition of sulfonated groups [42].

Fig. 6 displays the DSC curves of graphite oxide and rGO-SO<sub>3</sub>H samples. The DSC curves of graphite oxide and rGO-SO<sub>3</sub>H confirmed the results obtained by TGA analysis. The DSC curve of graphite oxide displays a broad peak at 170 °C, indicating the decomposition of thermally labile oxygen containing groups over the surface of graphite oxide. This peak is much decreased in DSC curve of rGO-SO<sub>3</sub>H (Fig. 6b), indicating that rGO-SO<sub>3</sub>H nanosheets are more stable than graphite oxide during heating.

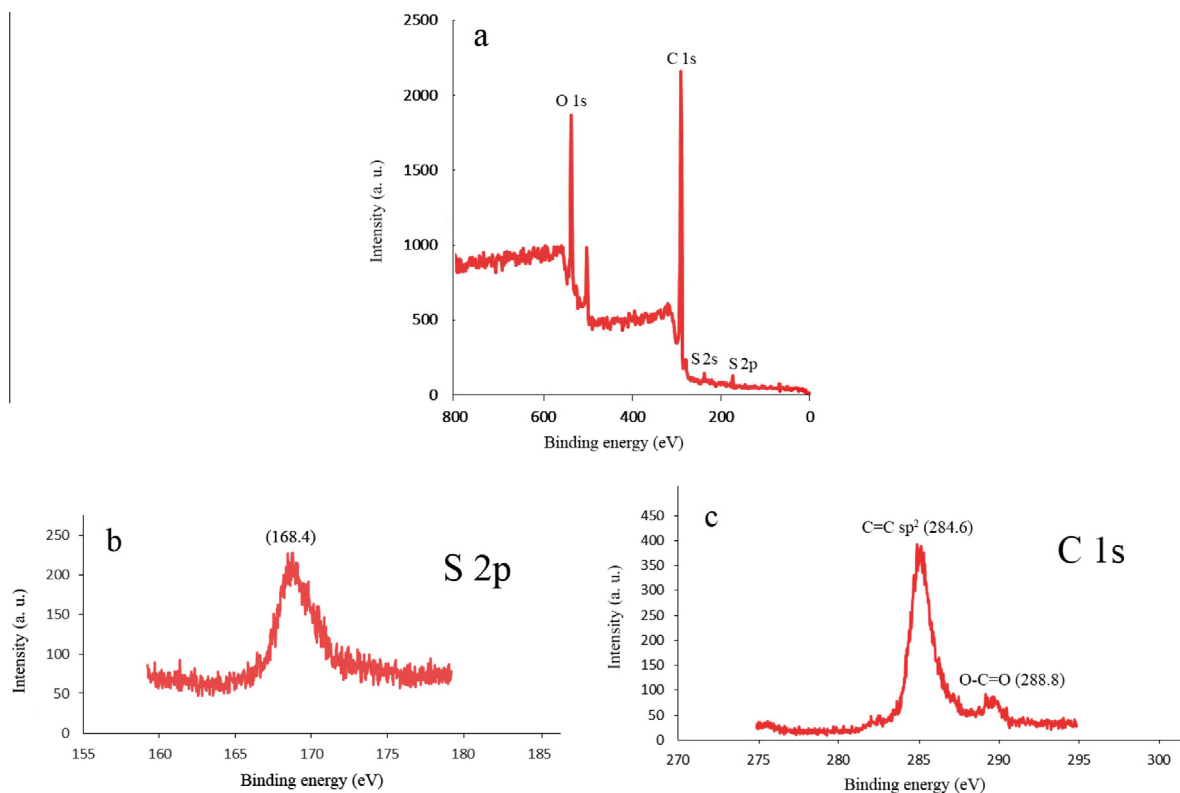


Fig. 7. (a) XPS wide-scan and high resolution spectra of (b) S<sub>2p</sub> and (c) C<sub>1s</sub> of rGO-SO<sub>3</sub>H nanosheets.

under otherwise similar experimental conditions (entry 8, Table 1). This result clearly supported the positive effect of rGO-SO<sub>3</sub>H catalyst on the amidation process. Similarly using graphite oxide as catalyst afforded *N*-phenylacetamide in 8% yield along with the starting material under ultrasonic irradiation (entry 9, Table 1). Finally, we examined the effect of a lower rGO-SO<sub>3</sub>H amount (2.5 mg) on the direct amidation of acetic acid with aniline (entry 10, Table 1). The results indicated that 5 mg of rGO-SO<sub>3</sub>H was optimum for this reaction.

Under the improved reaction conditions, direct amidation of various carboxylic acids with a variety of amines in the presence of rGO-SO<sub>3</sub>H (5 mg) under ultrasonic bath irradiation at room temperature gave the corresponding amides. The results are summarized in Table 2. Under these experimental conditions, the reaction of aniline, 4-chloroaniline, benzyl amine and *n*-propyl amine with acetic acid afforded the corresponding amides in 82–95% yields after 20–30 min. of sonication (entries 1–4, Table 2). Similarly, direct amidation of 4-chloroaniline, benzyl amine and morpholine with propionic acid using this method produced the corresponding amides in 76%, 80% and 73% yield, respectively under ultrasonic bath irradiation after 20 min. (entries 5–7, Table 2). Direct amidation of a carboxylic acid containing an electron-donating group such as 2-chloroacetic acid, with 4-chloroaniline and morpholine in presence of rGO-SO<sub>3</sub>H (5 mg) resulted in the formation of the corresponding amide derivatives in 81% and 75% yields, respectively after 20 min. (entries 8–9, Table 2). In the next step, we investigated the direct amidation of aromatic carboxylic acids such as benzoic acid and 4-nitrobenzoic acid with aromatic, hetero aromatic, cyclic and linear aliphatic amines under ultrasonic bath irradiation. *N*-(2,4-Dimethylphenyl)benzamide, *N*-(pyridin-4-yl)benzamide, morpholino(phenyl)methanone and 4-nitro-*N*-propylbenzamide were obtained in 92%, 85%, 80% and 94% yields, respectively in presence of rGO-SO<sub>3</sub>H after 20 min at room temperature (entries

Table 3  
Reusability of rGO-SO<sub>3</sub>H catalyst.

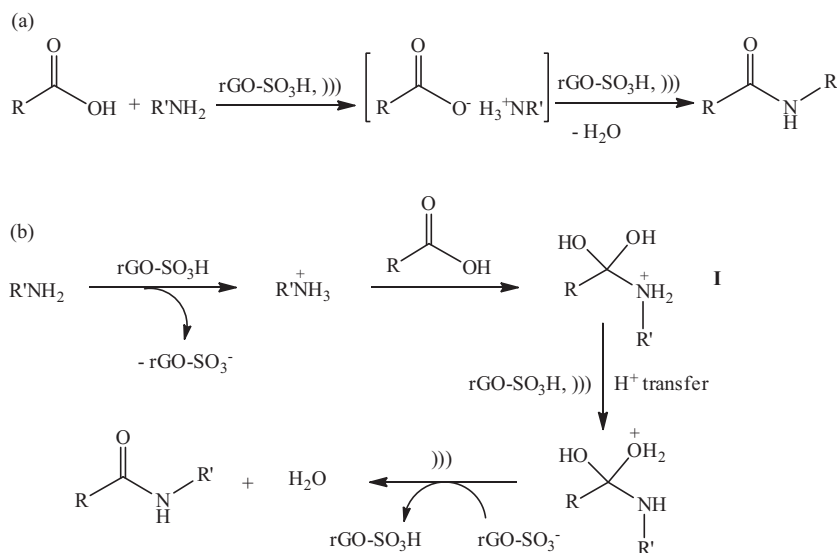
Run	1st	2nd	3rd	4th	5th	6th	7th
Yield <sup>a</sup> (%)	94	90	87	90	52 (90)	(88)	(89)

<sup>a</sup> The number in parentheses indicates the yield of amide by using the recycled acidified rGO-SO<sub>3</sub>H catalyst.

10–13, Table 2). Similarly, cinnamic acid reacted with morpholine to give the corresponding amide in 56% yield after 40 min sonication (entry 14, Table 2). Finally, we examined the direct sonochemical amidation of an hetero aromatic carboxylic acid, isonicotinic acid, with aniline, 2,4-dimethylaniline and *n*-propyl amine using rGO-SO<sub>3</sub>H catalyst under ultrasonic bath irradiation. The corresponding amides were obtained in 73%, 81% and 84% yields after 40 min. (entries 15–17, Table 2). The results indicated that through a sonochemical reaction, direct amidation of aliphatic, aromatic and hetero aromatic carboxylic acids with aromatic, benzylic, hetero aromatic, linear and cyclic aliphatic amines produced the corresponding amides in good to high yield in presence of rGO-SO<sub>3</sub>H catalyst in short reaction times at room temperature.

The results, obtained using this procedure, are comparable to those reported in the literature [5,9,12]. For example, Allen et al. [5] prepared *N*-benzylpropionamide in 81% yield by the reaction of propionic acid with benzyl amine in presence of 5 mol% ZrCl<sub>4</sub> in toluene at 110 °C for 5 h. *N*-(4-chlorophenyl)propionamide was synthesized by C–N coupling of propionamide to aryl halides in 94% yield using 5 mol% CuI catalyst in presence of 10 mol% *N,N'*-dimethylethylene diamine and 2–2.5 eq. cesium fluoride in tetrahydrofuran as solvent at room temperature after 18–24 h [12].

To evaluate the reusability of the rGO-SO<sub>3</sub>H catalyst after completion of the amidation reaction, ethyl acetate was added and the mixture was filtered through a sintered funnel to recover the catalyst. The reaction of acetic acid and aniline in the presence of



**Scheme 2.** Proposed mechanism for direct amidation of carboxylic acids with amines catalyzed by rGO-SO<sub>3</sub>H.

5 mg of the recovered rGO-SO<sub>3</sub>H was performed for five consecutive cycles. The recycled rGO-SO<sub>3</sub>H was efficient for the direct amidation of acetic acid into the corresponding amide even after four consecutive times (Table 3). However we observed a loss of activity of catalyst after the 5th run; the corresponding amide was obtained in 52% yield. Thus, the obtained recycled rGO-SO<sub>3</sub>H after 4th run was washed with a solution of hydrogen chloride (10%) and water, and centrifuged in water (3 times) for 20 min at 3700 rpm and then filtered and dried in an oven at 80 °C for 2 h. The recycled acidified rGO-SO<sub>3</sub>H was efficient for the direct amidation of acetic acid with aniline into the corresponding amide after seven consecutive cycles (Table 3).

#### 4. Mechanism

In addition to providing mechanical effects, cavitation induced by ultrasound can support many homogeneous and heterogeneous reactions. The basis of many applications of ultrasound is acoustic cavitation. The formation, growth and collapse of microbubbles generate high local pressure and release of heat energy. The result is an important increase of temperature and pressure of up to several thousand degrees Kelvin and several hundred bars. It is assumed that this cavitation bubble collapse provides the essential energy for a chemical reaction. The mechanism of direct amidation of carboxylic acids with amines using rGO-SO<sub>3</sub>H catalyst under ultrasonic irradiation is not very clear. However, a reasonable and appropriate mechanism is suggested for this reaction, as outlined in Scheme 2. The reaction may proceed through the initial formation of a stable ammonium carboxylate salt (Scheme 2a). This salt can undergo a subsequent dehydration leading to the formation of amide product [56]. Effect of ultrasound and high acid capacity of rGO-SO<sub>3</sub>H catalyst enhanced the formation of the ammonium carboxylate salt and the dehydration step. However, the reaction can proceed *via* pathway (b). In this pathway, high acid capacity of rGO-SO<sub>3</sub>H catalyst leads to the conversion of amine into ammonium salt. The intermediate I, obtained from the reaction between ammonium salt and carboxylic acid, undergoes a subsequent proton transfer leading to the formation of amide bond and water elimination [57]. Effect of ultrasound and high acid capacity of rGO-SO<sub>3</sub>H catalyst enhanced the proton transfer and the dehydration step.

#### 5. Conclusion

In conclusion, a simple technique was used to synthesize rGO-SO<sub>3</sub>H nanosheets by grafting sulfonic acid-containing aryl radicals onto rGO under sonochemical conditions. Through a sonochemical reaction we successfully achieved direct amidation of various carboxylic acids with a variety of amines using rGO-SO<sub>3</sub>H as a reusable solid acid catalyst. This new and simple ultrasonic procedure is advantageous as the amidation takes place at room temperature, in short reaction times and in good to high yields, reusable catalyst for seven consecutive cycles with a very simple work-up procedure.

#### Acknowledgment

The authors would like to thank the Iran National Science Foundation (INSF) for financial support.

#### References

- [1] A. Greenberg, C.M. Breneman, J.F. Liebman, *The Amide Linkage: Structural Significance in Chemistry, Biochemistry, and Materials Science*, John Wiley & Sons, 2000.
- [2] C. Lamberth, H.J. Kempf, M. Križ, *Synthesis and fungicidal activity of N-2-(3-methoxy-4-propargyloxy) phenethyl amides. Part 3: stretched and heterocyclic mandelamide oomycetocides*, *Pest Manag. Sci.* 63 (2007) 57–62.
- [3] H.M.D. Navickiene, J.E. Miranda, S.A. Bortoli, M.J. Kato, V.S. Bolzani, M. Furlan, *Toxicity of extracts and isobutyl amides from Piper tuberculatum: potent compounds with potential for the control of the velvetbean caterpillar, Anticarsia gemmatilis*, *Pest Manag. Sci.* 63 (2007) 399–403.
- [4] F. Xiao, Y. Liu, C. Tang, G.-J. Deng, *Peroxide-mediated transition-metal-free direct amidation of alcohols with nitroarenes*, *Org. Lett.* 14 (2012) 984–987.
- [5] C.L. Allen, A.R. Chhatwal, J.M. Williams, *Direct amide formation from unactivated carboxylic acids and amines*, *Chem. Commun.* 48 (2012) 666–668.
- [6] M.V. Khedkar, T. Sasaki, B.M. Bhanage, *Immobilized palladium metal-containing ionic liquid-catalyzed alkoxycarbonylation, phenoxycarbonylation, and aminocarbonylation reactions*, *ACS Catal.* 3 (2013) 287–293.
- [7] Q. Han, X. Xiong, S. Li, *An efficient, green and scale-up synthesis of amides from esters and amines catalyzed by Ru-MACHO catalyst under mild conditions*, *Catal. Commun.* 58 (2015) 85–88.
- [8] H. Prasad, G. Srinivasa, D. Channe Gowda, *Convenient, cost-effective, and mild method for the N-acetylation of anilines and secondary amines*, *Synth. Commun.* 35 (2005) 1189–1195.
- [9] C.L. Allen, S. Davulcu, J.M. Williams, *Catalytic acylation of amines with aldehydes or aldoximes*, *Org. Lett.* 12 (2010) 5096–5099.
- [10] S. Çalimsız, M.A. Lipton, *Synthesis of N-Fmoc-(2S,3S,4R)-3,4-dimethylglutamine: an application of lanthanide-catalyzed transamidation*, *J. Org. Chem.* 70 (2005) 6218–6221.

- [11] N.A. Stephenson, J. Zhu, S.H. Gellman, S.S. Stahl, Catalytic transamidation reactions compatible with tertiary amide metathesis under ambient conditions, *J. Am. Chem. Soc.* 131 (2009) 10003–10008.
- [12] D.P. Phillips, X.-F. Zhu, T.L. Lau, X. He, K. Yang, H. Liu, Copper-catalyzed C–N coupling of amides and nitrogen-containing heterocycles in the presence of cesium fluoride, *Tetrahedron Lett.* 50 (2009) 7293–7296.
- [13] A. Brennfürer, H. Neumann, M. Beller, Palladium-catalyzed carbonylation reactions of aryl halides and related compounds, *Angew. Chem. Int. Ed.* 48 (2009) 4114–4133.
- [14] S.-M. Lu, H. Alper, Sequence of intramolecular carbonylation and asymmetric hydrogenation reactions: highly regio- and enantioselective synthesis of medium ring tricyclic lactams, *J. Am. Chem. Soc.* 130 (2008) 6451–6455.
- [15] Z. Hu, S. Luo, Q. Zhu, Palladium-catalyzed intermolecular CH amidation of indoles with sulfonyl azides, *Sci. China Chem.* (2015) 1–5.
- [16] L. El Kaim, L. Grimaud, Beyond the Ugi reaction: less conventional interactions between isocyanides and iminium species, *Tetrahedron* 65 (2009) 2153–2171.
- [17] A. Alanthadka, C.U. Maheswari, N-Heterocyclic carbene-catalyzed oxidative amidation of aldehydes with amines, *Adv. Synth. Catal.* 357 (2015) 1199–1203.
- [18] X. Bantreil, C. Fleith, J. Martinez, F. Lamaty, Copper-catalyzed direct synthesis of benzamides from alcohols and amines, *ChemCatChem* 4 (2012) 1922–1925.
- [19] X.F. Wu, M. Sharif, A. Pews-Davtyan, P. Langer, K. Ayub, M. Beller, The first ZnII-catalyzed oxidative amidation of benzyl alcohols with amines under solvent-free conditions, *Eur. J. Org. Chem.* 2013 (2013) 2783–2787.
- [20] V. Polshettiwar, R.S. Varma, Green chemistry by nano-catalysis, *Green Chem.* 12 (2010) 743–754.
- [21] S.C. Ghosh, J.S. Ngiam, A.M. Seayad, D.T. Tuan, C.W. Johannes, A. Chen, Tandem oxidative amidation of benzyl alcohols with amine hydrochloride salts catalysed by iron nitrate, *Tetrahedron Lett.* 54 (2013) 4922–4925.
- [22] T. Wang, L. Yuan, Z. Zhao, A. Shao, M. Gao, Y. Huang, F. Xiong, H. Zhang, J. Zhao, Direct oxidative amidation between methylarenes and amines in water, *Green Chem.* 17 (2015) 2741–2744.
- [23] M. Kitano, K. Nakajima, J.N. Kondo, S. Hayashi, M. Hara, Protonated titanate nanotubes as solid acid catalyst, *J. Am. Chem. Soc.* 132 (2010) 6622–6623.
- [24] H.I. Ryo, L.Y. Hong, S.H. Jung, D.-P. Kim, Direct syntheses of sulfonated mesoporous SiO<sub>2</sub>-TiO<sub>2</sub>-SO<sub>3</sub>H materials as solid acid catalysts, *J. Mater. Chem.* 20 (2010) 6419–6421.
- [25] K. Nakajima, M. Hara, Amorphous carbon with SO<sub>3</sub>H groups as a solid Brønsted acid catalyst, *ACS Catal.* 2 (2012) 1296–1304.
- [26] R.T. Mayes, P.F. Fulvio, Z. Ma, S. Dai, Phosphorylated mesoporous carbon as a solid acid catalyst, *Phys. Chem. Chem. Phys.* 13 (2011) 2492–2494.
- [27] M. Spiro, Catalysis by carbons of reactions in solution, *Catal. Today* 7 (1990) 167–178.
- [28] S.K. Srivastava, J. Pionteck, Recent advances in preparation, structure, properties and applications of graphite oxide, *J. Nanosci. Nanotechnol.* 15 (2015) 1984–2000.
- [29] M. Mirza-Aghayan, R. Boukherroub, M. Nemat, M. Rahimifard, Graphite oxide mediated oxidative aromatization of 1,4-dihydropyridines into pyridine derivatives, *Tetrahedron Lett.* 53 (2012) 2473–2475.
- [30] M. Mirza-Aghayan, E. Kashef-Azar, R. Boukherroub, Graphite oxide: an efficient reagent for oxidation of alcohols under sonication, *Tetrahedron Lett.* 53 (2012) 4962–4965.
- [31] M. Mirza-Aghayan, M.M. Tavana, R. Boukherroub, Oxone/iron (II) sulfate/graphite oxide as a highly effective system for oxidation of alcohols under ultrasonic irradiation, *Tetrahedron Lett.* 55 (2014) 342–345.
- [32] M. Mirza-Aghayan, S. Zonoubi, M.M. Tavana, R. Boukherroub, Ultrasound assisted direct oxidative esterification of aldehydes and alcohols using graphite oxide and oxone, *Ultrason. Sonochem.* 22 (2015) 359–364.
- [33] M. Mirza-Aghayan, R. Boukherroub, M. Rahimifard, Graphite oxide as an efficient solid reagent for esterification reactions, *Turk. J. Chem.* 38 (2014) 859–864.
- [34] M. Mirza-Aghayan, M. Alizadeh, M.M. Tavana, R. Boukherroub, Graphite oxide: a simple and efficient solid acid catalyst for the ring-opening of epoxides by alcohols, *Tetrahedron Lett.* 55 (2014) 6694–6697.
- [35] S.S. Maktedar, S.S. Mehetre, M. Singh, R.K. Kale, Ultrasound irradiation: a robust approach for direct functionalization of graphene oxide with thermal and antimicrobial aspects, *Ultrason. Sonochem.* 21 (2014) 1407–1416.
- [36] L. Wang, D. Wang, S. Zhang, H. Tian, Synthesis and characterization of sulfonated graphene as a highly active solid acid catalyst for the ester-exchange reaction, *Catal. Sci. Technol.* 3 (2013) 1194–1197.
- [37] J. Zhou, Y. Wang, X. Guo, J. Mao, S. Zhang, Etherification of glycerol with isobutene on sulfonated graphene: reaction and separation, *Green Chem.* 16 (2014) 4669–4679.
- [38] G. Cravotto, P. Cintas, Power ultrasound in organic synthesis: moving cavitation chemistry from academia to innovative and large-scale applications, *Chem. Soc. Rev.* 35 (2006) 180–196.
- [39] S. Li, W. Meng, X. Fu, L. Liu, J. Zhang, C. Cheng, N. Lan, W. Cui, Y. Liu, An efficient and practical synthesis of ropivacaine hydrochloride under ultrasound irradiation, *Lat. Am. J. Pharm.* 32 (2013) 1258–1262.
- [40] A. Dandia, D. Bhati, A. Jain, G. Sharma, Ultrasound promoted clay catalyzed efficient and one pot synthesis of substituted oxindoles, *Ultrason. Sonochem.* 18 (2011) 1143–1147.
- [41] M.S. Ardestani, A.J. Arabzadeh, Z. Heidari, A. Hosseinzadeh, H. Ebrahimi, E. Hashemi, M. Mosayebnia, M. Shafiee-Alavidjeh, A. Alavi, M.H. Babaei, Novel and facile methods for the synthesis of DTPA-mono-amide: a new completely revised strategy in radiopharmaceutical chemistry, *J. Radioanal. Nucl. Chem.* 283 (2010) 447–455.
- [42] Y. Wang, Y. Zhao, W. He, J. Yin, Y. Su, Palladium nanoparticles supported on reduced graphene oxide: facile synthesis and highly efficient electrocatalytic performance for methanol oxidation, *Thin Solid Films* 544 (2013) 88–92.
- [43] M. Mirza-Aghayan, M.M. Tavana, R. Boukherroub, Palladium nanoparticles supported on reduced graphene oxide as an efficient catalyst for the reduction of benzyl alcohol compounds, *Catal. Commun.* 69 (2015) 97–103.
- [44] D. He, Z. Kou, Y. Xiong, K. Cheng, X. Chen, M. Pan, S. Mu, Simultaneous sulfonation and reduction of graphene oxide as highly efficient supports for metal nanocatalysts, *Carbon* 66 (2014) 312–319.
- [45] H. Naeimi, M. Golestanzadeh, Microwave-assisted synthesis of 6,6'-(aryl (alkyl) methylene) bis (2,4-dialkylphenol) antioxidants catalyzed by multi-sulfonated reduced graphene oxide nanosheets in water, *New J. Chem.* 39 (2015) 2697–2710.
- [46] E. Lam, J.H. Chong, E. Majid, Y. Liu, S. Hrapovic, A.C.W. Leung, J.H.T. Luong, Carboxylic acid-catalyzed dehydration of xylose to furfural in water, *Carbon* 50 (2012) 1033–1043.
- [47] V. Thanh, J. Demelza, A novel aromatic carbocation-based coupling reagent for esterification and amidation reactions, *Chem. Commun.* 51 (2015) 3131–3134.
- [48] S.R. Narahari, B.R. Reguri, K. Mukkanti, Beckmann rearrangement of oximes using pivaloyl chloride/DMF complex, *Tetrahedron Lett.* 52 (2011) 4888–4891.
- [49] S.-K. Yang, J.S. Kang, P. Oelschlaeger, K.-W. Yang, Azolythioacetamide: a highly promising scaffold for the development of metallo-β-lactamase inhibitors, *ACS Med. Chem.* 6 (2015) 455–460.
- [50] J. Pielichowski, R. Popielarz, Trichloroethylene in organic synthesis: II. Reaction of trichloroethylene with secondary amines, *Tetrahedron* 40 (1984) 2671–2675.
- [51] M. Ashif Ali, P. Saha, T. Punniyamurthy, Efficient copper-catalyzed N-arylation of amides and imidazoles with aryl iodides, *Synthesis* (2010) 908–910.
- [52] J.L. Vrijdag, F. Delgado, N. Alonso, W.M. De Borggraeve, N. Pérez-Macias, J. Alcázar, Practical preparation of challenging amides from non-nucleophilic amines and esters under flow conditions, *Chem. Commun.* 50 (2014) 15094–15097.
- [53] V. Štrukil, B. Bartolec, T. Portada, I. Dilović, I. Halasz, D. Margetić, One-pot mechanosynthesis of aromatic amides and dipeptides from carboxylic acids and amines, *Chem. Commun.* 48 (2012) 12100–12102.
- [54] R.D.C. Rodrigues, I.M. Barros, E.L. Lima, Mild one-pot conversion of carboxylic acids to amides or esters with Ph3P/trichloroisocyanuric acid, *Tetrahedron Lett.* 46 (2005) 5945–5947.
- [55] S. Korom, P. Ballester, Pyridyl-decorated self-folding heptaamide cavitands as ligands in the rhodium-catalyzed hydrogenation of norbornadiene, *Eur. J. Org. Chem.* 2014 (2014) 4276–4282.
- [56] N. Gernigon, R.M. Al-Zoubi, D.G. Hall, Direct amidation of carboxylic acids catalyzed by ortho-iodo arylboronic acids: catalyst optimization, scope, and preliminary mechanistic study supporting a peculiar halogen acceleration effect, *J. Org. Chem.* 77 (2012) 8386–8400.
- [57] F. Arena, C. Deiana, A.F. Lombardo, P. Ivanchenko, Y. Sakhno, G. Trunfio, G. Martra, Activity patterns of metal oxide catalysts in the synthesis of N-phenylpropionamide from propanoic acid and aniline, *Catal. Sci. Technol.* 5 (2015) 1911–1918.